## Near fields and far fields generated by sources in the presence of dielectric structures with cylindrical symmetry

Soendergaard, T.; Lenstra, D.; Tromborg, B.

***published in***
Optics Letters
2001

***DOI (link to publisher)***
10.1364/OL.26.001705

***document version***
Publisher's PDF, also known as Version of record

# Near fields and far fields generated by sources in the presence of dielectric structures with cylindrical symmetry

**T. Søndergaard**

*Vrije Universiteit, De Boelelaan 1081, 1081 HV Amsterdam, The Netherlands, and COM, Technical University of Denmark, Building 345, DK-2800 Kgs. Lyngby, Denmark*

**D. Lenstra**

*Vrije Universiteit, De Boelelaan 1081, 1081 HV Amsterdam, The Netherlands*

**B. Tromborg**

*COM, Technical University of Denmark, Building 345, DK-2800 Kgs. Lyngby, Denmark*

Received April 23, 2001

A full-vectorial integral equation method is presented for calculating near fields and far fields generated by sources in the presence of general finite-sized dielectric structures with cylindrical symmetry. The method is relevant for modeling of a class of antenna designs and some optical components with cylindrical symmetry, e.g., vertical-cavity surface-emitting lasers, microdisk lasers, and light-emitting diodes. 

*OCIS codes:* 130.0130, 250.2110, 000.3860.

We present a full-vectorial integral equation method for calculating electromagnetic near fields and far fields generated by sources in the presence of three-dimensional dielectric structures with cylindrical symmetry. The method presented is a further development of the integral equation approaches of, e.g., Purcell and Pennypacker,[1] Draine,[2] Martin *et al.*,[3] and Hoekstra *et al.*[4] to take advantage of cylindrical symmetry. Thereby the computational task is drastically reduced because the three-dimensional computational problem is reduced to a series of two-dimensional problems. One calculation must be performed for each angular-momentum component of the field. Furthermore, unlike in previous research,[1–4] we introduce fields generated by current sources. This makes it feasible to calculate both near and far fields generated by a distribution of currents inside, e.g., vertical-cavity surface-emitting lasers, microdisk lasers, and light-emitting diodes.

The electric field generated by a distribution of currents $\mathbf{J}(\mathbf{r})$ is generally given as the retarded solution to the inhomogeneous wave equation in the frequency domain:

$$-\nabla \times \nabla \times \mathbf{E}(\mathbf{r}) + k^2 \epsilon(\mathbf{r}) \cdot \mathbf{E}(\mathbf{r}) = -i\omega\mu \mathbf{J}(\mathbf{r}), \quad (1)$$

where $k$ is the free-space wave number, $\epsilon$ is the dielectric tensor, $\omega$ is the angular frequency, and $\mu$ is the vacuum permeability. The electric field solution can be expressed in terms of the currents and dyadic Green's tensor $\mathbf{G}$ of the structure, i.e.,

$$\mathbf{E}(\mathbf{r}) = i\omega\mu \int \mathbf{G}(\mathbf{r},\mathbf{r}') \cdot \mathbf{J}(\mathbf{r}')\mathrm{d}^3 r', \quad (2)$$

where $\mathbf{G}$ is the retarded solution to

$$-\nabla \times \nabla \times \mathbf{G}(\mathbf{r},\mathbf{r}') + k^2 \epsilon(\mathbf{r}) \cdot \mathbf{G}(\mathbf{r},\mathbf{r}') = -\mathbf{I}\delta(\mathbf{r}-\mathbf{r}'). \quad (3)$$

Here $\mathbf{I}$ is the unit tensor and $\delta$ is the Dirac delta function.

We take advantage of the following identity between Green's tensor $\mathbf{G}$ for the structure with dielectric tensor $\epsilon$ and free-space Green's tensor $\mathbf{G}^0$:

$$\mathbf{G}(\mathbf{r},\mathbf{r}') = \mathbf{G}^0(\mathbf{r},\mathbf{r}') + k^2 \int \mathbf{G}^0(\mathbf{r},\mathbf{r}'') \cdot [\epsilon(\mathbf{r}'') - \mathbf{I}] \cdot \mathbf{G}(\mathbf{r}'',\mathbf{r}')\mathrm{d}^3 r''. \quad (4)$$

By substitution of Eq. (4) into Eq. (2) we find a Lippmann–Schwinger-type integral equation for the electric field generated by the distribution of currents $\mathbf{J}(\mathbf{r})$, where the effect of the sources enters via the field $\mathbf{E}^0$ that these sources would have generated in free space; i.e.,

$$\mathbf{E}(\mathbf{r}) = \mathbf{E}^0(\mathbf{r}) + k^2 \int \mathbf{G}^0(\mathbf{r},\mathbf{r}') \cdot [\epsilon(\mathbf{r}') - \mathbf{I}] \cdot \mathbf{E}(\mathbf{r}')\mathrm{d}^3 r'. \quad (5)$$

Previously an equation of this type was solved by Purcell and Pennypacker,[1] Draine,[2] Martin *et al.*,[3] and Hoekstra *et al.*,[4] who discretized the dielectric structure of interest into cubic volume elements, where the fields $\mathbf{E}$ and $\mathbf{E}^0$ were assumed constant within each volume element. In their case the field $\mathbf{E}^0$ was a solution to the homogeneous wave equation, i.e., Eq. (1), with $\epsilon = \mathbf{I}$ and $\mathbf{J} = \mathbf{0}$. When a dipole current source is considered, solving Eq. (5) is equivalent to calculating elements of Green's tensor $\mathbf{G}$.

For dielectric structures with cylindrical symmetry a discretization approach based on ring volume elements is more appropriate than the use of cubic volume elements. First, fields $\mathbf{E}$ and $\mathbf{E}^0$ are expanded in angular-momentum components in the form

$$\mathbf{E}^m\mathbf{r}() = [\hat{z}E_z^m(\rho,z) + \hat{\rho}E_\rho^m(\rho,z) + \hat{\phi}E_\phi^m(\rho,z)]\exp(im\phi), \quad (6)$$

 

where $\hat{\rho}$, $\hat{\phi}$, $\hat{z}$ and $\rho$, $\phi$, $z$ are the coordinate unit vectors and the position coordinates, respectively, in a cylindrical coordinate system. For fields in this form it is sufficient to discretize the field components $E_z^m$, $E_\rho^m$, and $E_\phi^m$ in $\rho$ and $z$, thereby reducing the three-dimensional problem to a two-dimensional problem. The structure is also discretized in $\rho$ and $z$, i.e., in ring volume elements. The discretized Lippmann–Schwinger equation may then be written as

$$E_{p,i}^m - \sum_j \sum_{q,s=\rho,\phi,z} G_{pq,ij}^m k^2(\epsilon_{qs,j} - \delta_{qs})E_{s,j}^m = E_{p,i}^{0,m}\,, \tag{7}$$

where $\delta_{qs}$ is the Kronecker delta function and

$$G_{pq,ij}^m = \int_{\text{ring elem } j} \hat{\mathrm{p}} \cdot \mathbf{G}^0(\mathbf{r}_i, \mathbf{r}') \cdot \hat{q}' \exp[im(\phi' - \phi)]\mathrm{d}^3 r'. \tag{8}$$

Note that, whereas the direction of $\hat{\rho}$ and $\hat{\phi}$ is determined by angle $\phi$, the direction of $\hat{\rho}'$ and $\hat{\phi}'$ is determined by angle $\phi'$ ($\hat{z}' = \hat{z}$). Using a dielectric tensor in Eq. (7) rather than a scalar adds some complexity, but the tensor permits interpolation by effective-medium theory in the style of Meade *et al.*,[5] leading to a drastically improved representation of the dielectric structure when the structure is discretized. For the special case when $i = j$ the matrix element in Eq. (8) requires integration over the singularity of the Green's tensor. For cubic volume elements it is possible for quite small discretization elements to circumvent this integration by use of the Clausius–Mossotti relation[1] or by use of the tabulations for the more-general volume elements given by Yaghjian.[6] It is not practical to use such small volume elements[3]; also, in our case the field cannot generally be assumed constant within a ring volume element [there is, e.g., the phase factor $\exp(im\phi)$]. Therefore we adopt the method of Nachamkin[7] to perform part of the integration as a surface integral away from the point of singularity, i.e.,

$$\begin{aligned} k^2 G_{pq,ij}^m = {}& k^2 \int_{\text{ring elem } i} \hat{\rho} \cdot \mathbf{G}^0(\mathbf{r}_i, \mathbf{r}') \cdot \{\hat{q}' \exp[im(\phi' \\ & - \phi)] - \hat{q}\}\mathrm{d}^3 r' - \delta_{pq} + \oint_{\substack{\text{surf of}\\ \text{ring elem } i}} \hat{\rho} \cdot [-\mathbf{I}(\nabla_{\mathbf{R}'} g \cdot \hat{n}) \\ & + \hat{n}(\nabla_{\mathbf{R}'} g)] \cdot \hat{q}\mathrm{d}^2 r', \end{aligned} \tag{9}$$

where $\mathbf{R}' = \mathbf{r}' - \mathbf{r}$, $\hat{n}$ is the unit outward surface-normal vector, and $g$ is the scalar Green's function, defined by

$$g(\mathbf{r}, \mathbf{r}') = \frac{\exp(ik|\mathbf{r} - \mathbf{r}'|)}{4\pi|\mathbf{r} - \mathbf{r}'|}\cdot \tag{10}$$

Equation (7) is solved by use of a conjugate gradient algorithm similar to the one used by Draine.[2]

A major advantage of the method for finite structures is that we can restrict our computational domain to the region where $(\epsilon - \mathbf{I})$ is nonzero. Using Eq. (5) or Eq. (7), we can straightforwardly calculate the field at any point outside the dielectric structure once the field inside the structure is known.

The method has been tested against both numerical and analytic results. First we used the approach of Martin *et al.*[3] based on cubic volume elements to calculate a number of near and far fields for structures with cylindrical symmetry. Calculations with our approach that take advantage of cylindrical symmetry give similar or better results when the same resolution per dimension is used (it is of course difficult to represent cylindrical objects properly with cubic volume elements). The method has also been tested against analytical results from Mie scattering theory[2,8] for extinction efficiency and absorption efficiency for a plane wave incident upon an absorbing dielectric sphere. The extinction and absorption efficiencies are measures of how efficiently light is lost from the incident beam of light as a result of scattering and absorption. Compared with the results of tests by Draine based on cubic volume elements, we obtain similar convergence by using typically 20 times fewer discretization elements.

The strength of our method is of course that it can be applied to a number of structures for which analytical calculations are not possible. In Figs. 1 and 2 we consider a dipole current source polarized along the $x$ axis in the center of a dielectric ring with refractive index $n = 3.5$ (GaAs), height 137 nm, outer diameter 1600 nm, and width 650 nm. The dipole emission wavelength is $\lambda = 1000$ nm, and thereby the height of the ring is approximately one half-wavelength in the medium. We performed the calculations in this Letter by resolving the structure in the $\rho z$ plane in elements of size 12.5 nm × 12.5 nm.

The amplitude of the electric field in the $yz$ plane generated by the dipole current in the presence of the ring is shown as a contour plot in Fig. 1. The

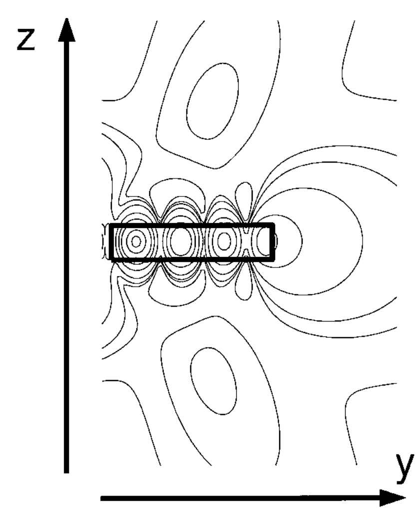


Fig. 1. Amplitude of the electric field generated by a dipole polarized along the $x$ axis in the center of a dielectric ring with refractive index 3.5, height 137 nm, outer diameter 1600 nm, and width 650 nm.

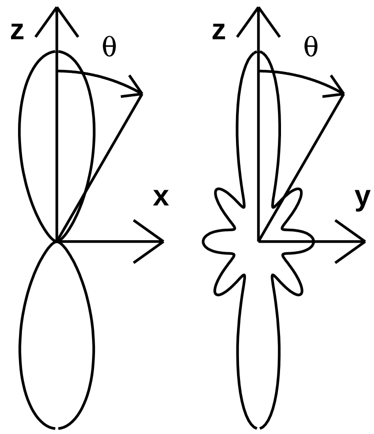


Fig. 2. Far-field off-axis angular radiation patterns generated by a dipole polarized along the $x$ axis in the center of a dielectric ring with refractive index 3.5, height 137 nm, outer diameter 1600 nm, and width 650 nm.

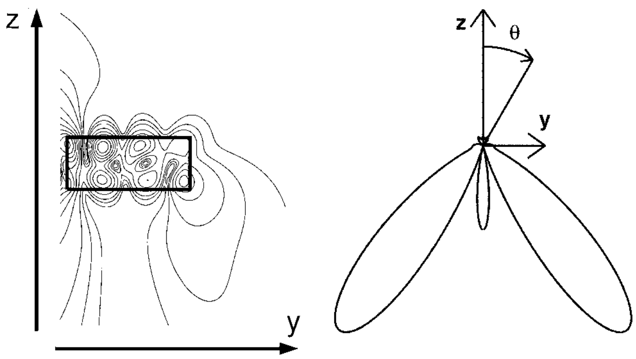


Fig. 3. Near field and far field generated by a dipole polarized along the $x$ axis positioned on the $z$ axis 70 nm inside a dielectric ring, measured from the bottom of the ring, with refractive index 3.5, height 275 nm, outer diameter 1600 nm, and width 650 nm.

lightest areas show high amplitude; black, low (zero) amplitude. The field in this plane is particularly illustrative because here it is continuous across all dielectric interfaces, and it is also in this plane that the presence of the dielectric ring results in the most significant modifications of the dipole emission pattern. The cross section of the ring is shown in Fig. 1 enclosed by a black rectangular box. The field is not shown directly at the $z$ axis because the dipole field here is singular. Note the excitation of a standing-wave pattern in the ring along the $y$ axis and along the $z$ axis. The corresponding far-field off-axis angular radiation patterns are shown in Fig. 2. These patterns show the power flux $\mathrm{d}P$ of emitted light per unit solid angle $\mathrm{d}\Omega$, i.e.,

$$\frac{\mathrm{d}P}{\mathrm{d}\Omega} = \lim_{r\to\infty} r^2 |\mathbf{S}(\mathbf{r})|\,, \tag{11}$$

where $\mathbf{S}$ is the Poynting vector, which for large distances reduces to

$$\mathbf{S} = 2(\mathbf{r}/r)\epsilon_0 c|\mathbf{E}|^2. \tag{12}$$

Here $\epsilon_0$ is the vacuum permittivity and $c$ is the speed of light. We obtain the far-field radiation pattern by calculating the electric field at large distances, using Eq. (7). For the far-field patterns in Fig. 2 it is clear that for the $zx$ plane it is similar to the dipole pattern when the dielectric ring is not present; in free space the pattern is also a figure 8. For the $yz$ plane the far-field radiation pattern is significantly modified by the presence of the dielectric ring, because in free space it would have been a circle.

We give one more example of near and far fields in Fig. 3, where the height of the ring is now 275 nm. The dipole is still positioned at the $z$ axis and is polarized along the $x$ axis. It is now placed 70 nm inside the ring from the bottom. Because of the asymmetric dipole position, the near-field and far-field emission patterns also become asymmetric, and a large fraction of the emission is directed downward. Owing to the doubling of the ring height, the excited standing-wave pattern inside the ring along the $z$ axis is also more complex, with a minimum that is roughly in the middle of the pattern.

The method developed requires that the fields $\mathbf{E}$ and $\mathbf{E}^0$ can be assumed constant in $\rho$ and $z$ within each discretization element. This is the main reason why the dipole is not placed inside the dielectric, as this assumption does not hold for highly singular fields. However, when we consider a smoother distribution of currents that gives rise to nonsingular fields, it is also possible to consider fields emitted by currents placed inside the dielectric.

In conclusion, a method based on the discretized Lippmann–Schwinger integral equation has been presented for calculating near and far fields generated by sources in the presence of dielectric structures with cylindrical symmetry. The method was exemplified for a dipole current source in the center of a dielectric ring. In these examples it was possible to observe the excitation of standing-wave patterns inside the ring. The angular far-field radiation patterns permitted evaluation of the emitted intensity as a function of direction. The method has prospective uses for calculating near-field and far-field radiation patterns for a class of antenna designs and for some optical components with cylindrical symmetry, e.g., vertical-cavity surface-emitting lasers, microdisk lasers, and light-emitting diodes.

T. Søndergaard's e-mail address is ts@com.dtu.dk.

## References


1. E. M. Purcell and C. R. Pennypacker, Astrophys. J. **186,** 706 (1973).
2. B. T. Draine, Astrophys. J. **333,** 848 (1988).
3. O. J. F. Martin, C. Girard, and A. Dereux, Phys. Rev. Lett. **74,** 526 (1995).
4. A. Hoekstra, J. Rahola, and P. Sloot, Appl. Opt. **37,** 8482 (1998).
5. R. D. Meade, A. M. Rappe, K. D. Brommer, J. D. Joannopoulos, and O. L. Alerhand, Phys. Rev. B **48,** 8434 (1993).
6. A. D. Vaghjian, Proc. IEEE **68,** 243 (1980).
7. J. Nachamkin, IEEE Trans. Antennas Propag. **38,** 919 (1990).
8. G. Mie, Ann. Phys. (Leipzig) **25,** 377 (1880).